N° d'ordre : 4420 **ANNÉE 2012**

UNIVERSITÉ DE RENNES 1

ueb

THÈSE / UNIVERSITÉ DE RENNES 1
sous le sceau de l'Université Européenne de Bretagne

pour le grade de

DOCTEUR DE L'UNIVERSITÉ DE RENNES 1

Mention : Traitement du Signal et Télécommunications

Ecole doctorale Matisse

présentée par

Samsul Haimi DAHLAN

Préparée à l'unité de recherche (UMR CNRS 6164, IETR)
Institut d'Electronique et de Télécommunications de Rennes Université de Rennes 1

Contribution to the body of revolution finite-difference time domain (BoR-FDTD) method – Implementations of hybrid and multi-resolution approaches for fast simulation of electrically large axis-symmetrical antenna structures.

Thèse soutenue à l'Université de Rennes 1 le 13 Janvier 2012

devant le jury composé de :

Mme Elodie RICHALOT
Professeur des Universités, Université de Paris-Est / *rapporteur*

M. Michel NEY
Professeur, Télécom Bretagne / *rapporteur*

M. Alain REINEIX
Directeur de Recherche au CNRS, Université de Limoges / *examinateur*

M. Renaud LOISON
Professeur des Universités, INSA de Rennes / *examinateur*

M. Anthony ROLLAND
Docteur de l'Université de Rennes 1 / *examinateur*

M. Ronan SAULEAU
Professeur des Universités, Université de Rennes 1 / *directeur de thèse*

Appendix

Contribution to the body of revolution finite-difference time domain (BoR-FDTD) method – Implementations of hybrid and multi-resolution approaches for fast simulation of electrically large axis-symmetrical antenna structures

Table of contents

Chapter 1

General Introduction

1.1 History and collaboration

This Ph.D thesis on the Body-of-Revolution Finite-Difference Time-Domain (BoR-FDTD) was conducted at IETR (Institute of Electronics and Telecommunications of Rennes). It was supervised by Ronan SAULEAU (Professor at University Rennes 1). This work was supported in part by the "Université Européenne de Bretagne" and the "Conseil Régional de Bretagne" (project acronyms: OPTIMISE, CREATE/CONFOCAL and GRAPPAS) and UTHM (Universiti Tun Hussien Onn Malaysia) for the Ph.D scholarship.

The development of the BoR-FDTD simulator at IETR started in 2006 by Dr. Ming-Sze Tong. He contributed in the development of the kernel programs of the simulator and used it for electromagnetic study focusing on the electromagnetic band-gap structures (EBGs) in BoR environment [1], [2].

This work was then continued by Anthony Rolland, who defended his Ph.D in 2009. His thesis entitled "*Conception d'antennes métallo-diélectriques par optimisation globale basée sur le couplage entre la méthode FDTD et les algorithmes génétiques*" combines the BoR-FDTD simulator with an optimization technique which is based on the Genetic Algorithms (GA) for the synthesis and the development of dielectric and lens antennas with axis-symmetrical structure [3].

The BoR-FDTD is well known for fast and efficient method compared with the fully three-dimensional (3D) FDTD simulator. In this present work, we explore and introduce techniques to further reduce the computational effort especially for the simulation of large body-of-revolution structures using the BoR-FDTD method.

1.2 Contexts and Objectives of the study

During the last several years, electromagnetic simulators have become an essential and popular tools for the engineers and scientists in many engineering fields as well as for research and development (R&D) activities. The growing needs for these simulators is partly due to high demand for fast and efficient design tools, also as a result from the increasing complexity of modern devices where many of them were previously beyond the imaginations. Various applications today comes with stringent specifications and requirements, make it almost impossible to fulfill the job with previously old fashioned try-and-cut technique. Because of this, a lot of effort has been focused on the development of numerical methods and algorithms for various scientific disciplines.

One of the most popular numerical methods in electromagnetics is the Finite-Difference Time-Domain. The method was originally introduced by Kane Yee in 1966 and has been proved to be an accurate technique for the simulations of various electromagnetic problems [4]. In general, any electromagnetic structure can be possibly described in three-dimensional using the Cartesian coordinate system. Nevertheless, to have results with high accuracy this simulation normally required high computational efforts. For FDTD, this effort could be in the form of the utilization of high mesh resolutions which would lead to prohibitive memory requirements and consequently need unavoidable long computational time. Maybe the three dimensional (3-D) Cartesian FDTD is the most versatile technique for general solution of electromagnetic problems but it might not be the most effective. In many cases, the electromagnetic information about the structure can be extracted from fields in the space region. The use of the geometrical symmetry with respect to the principle planes of the coordinate system allows economizing computer resources when performing a simulation [5]. This includes simulation involving the axis-symmetrical structures or well known as the body of revolution.

The body-of-revolution structures such as the conical and corrugated horns are typically used for primary feeds of reflector antennas, or axis-symmetrical focusing systems based on reflectors and lenses. They are extremely attractive for microwave and millimeter waves applications since they are simple to fabricate. Their axial symmetrical structure leads to odd and even field distribution along azimuthal direction. In order to efficiently analyze such rotationally symmetric structures, an efficient and memory-saving FDTD algorithm,

called the BoR-FDTD method is used. It is a cylindrical coordinate based system, and it expands the φ-dependence of the fields using Fourier series. As a result, a three-dimensional (3-D) Yee's lattice in (ρ,φ,z) is projected onto a two-dimensional (2-D) ρ-z plane, accompanied with the mode number set in the Fourier series. Eventually, this field projection results in significant savings in terms of computational memory and time when compared with the full 3-D scheme [6].

The subject of this thesis focuses on the BoR-FDTD method for the study and simulation of several BoR antenna structures. It should be emphasized that the growing interest in the electromagnetic modeling especially for simulation of antenna and its environment often pushes the simulator beyond its computational capabilities. One of the possible solutions is to combine additional techniques and approaches into the original BoR-FDTD computational algorithm that could speed up the calculation for specific BoR problems without deteriorating the accuracy.

The objective of this thesis is to introduce and implement methods that can be efficiently used for the simulation of electrically large BoR structure. Two methods are proposed by means of hybrid technique and a method involving multi-grid resolution. Our BoR-FDTD combined with these techniques shows significantly better performance if compared with the classical BoR-FDTD method in terms of the computer resources utilizations when applied in the simulation of electrically large antenna structure.

Using the advantage of the fast simulation of the BoR-FDTD, a simulation study involving short circular ring loaded horn with minimized cross polarization (SCRIMP) horn antenna with utilizing the genetic-algorithm optimization tool was performed and the simulation results are presented.

1.3 Thesis overview

Chapter 2 presents a brief outline of the FDTD method, emphasizing its major advantages over the other modeling methods, but also pointing out its inherent limitations.

Chapter 3 details the algorithms used for the BoR-FDTD simulator. This chapter covers the governing equations and steps taken to discretize them for used in the FDTD method. The trick to handle the singularity of field components along the axis of rotation is also discussed in detail. To truncate the simulation space to infinity the uniaxial perfectly matched layer (U-PML) is used and the implementations including the equations are briefly outlined. Several possible excitations mode including the TEM, TE and TM are discussed. Tools for the analysis of antennas including the near-field to far-field transformation, power and directivity calculations, reflection coefficient as well as the total-field/scattered field technique are explained. Finally the work flow of the BoR-FDTD simulator is presented.

Chapter 4 presents applications of the BoR-FDTD simulator in the simulation of BoR antennas. In particular, the chapter discussed on the analysis and designs of the SCRIMP horn antenna. The optimization tool based on the genetic algorithm (GA) (previously developed at IETR) is used for optimization of the SCRIMP horn. Finally several optimized SCRIMP horn designs are proposed in S and C-bands.

Chapter 5 introduces a hybrid technique for the BoR-FDTD solver. It combines the solver with the field transformation technique based on the Kirchoff surface integral formulation for determining fields in near- and far-field region inside the BoR-FDTD domain. The derivation of the equation is detailed in this chapter, and the implementation is explained. New method for fast simulation of large BoR structure such as the reflector antenna system is introduced. It is called the dual-region scheme (DR-BoR-FDTD). Several parametric study approaches for reflector antennas by using the DR-BoR-FDTD are presented. Advantages and limitations of the technique and approach to enhance its capabilities are then addressed.

Chapter 6 presents a new multi-resolution technique for used with the BoR-FDTD solver. The technique known as the dual-grid (DG-BoR-FDTD) combines two successive simulations using different grid sizes for solving electrically large BoR structure using the BoR-FDTD. This technique has been proposed in Cartesian coordinates by IETR [10], and is extended here for bodies of revolutions. The implementation is described in detail with

emphasis on the mechanisms used to link the two separate BoR-FDTD volumes, namely the sampling or interpolation in time and space, and the TF/SF decomposition. The set of general equations has been derived for any mesh ratio value. In addition, a technique to calculate accurately the antenna reflection coefficient due to combinations of two separate BoR-FDTD volumes with different mesh resolution is introduced, and the equation is derived. The proposed technique is validated with several reflector antenna systems, and the performance is compared with classical BoR-FDTD run.

1.4 Original contributions

This thesis presents the author's original contributions in the following area:

- Simulation study and analysis of SCRIMP horn antenna using the BoR-FDTD (Chapter 4).
- Derivation and implementation of Kirchoff surface integral equation in cylindrical coordinate system for used in BoR-FDTD method (Chapter 5).
- Implementation and evaluation of the near-field to near-field (NFNF) transformation based on the surface integration technique in BoR-FDTD (Chapter 5).
- Development, implementation and evaluation of a hybrid scheme for electrically large BoR structure simulation in BoR-FDTD (Chapter 5).
- Development, implementation and evaluation of a multi-resolution scheme based on the dual-grid technique (DG-BoR-FDTD) in the BoR-FDTD (Chapter 6).
- Derivation and implementation of the space and time interpolation technique for used with the DG-BoR-FDTD (Chapter 6).
- Derivation, implementation and evaluation of a correction technique for the calculation of reflection coefficient S_{11} used with the DG-BoR-FDTD (Chapter 6).

Several conference papers have been published from this work [7], [8], [9]. A journal on the multi-resolution technique used in this work is currently under review.

References

[1] Ming Sze Tong, "Final report on body-of-revolution FDTD," (Unpublished)

[2] M. –S. Tong, R. Sauleau, A. Rolland, and T.-G. Chang, "Analysis of Electromagnetic Band-Gap (EBG) waveguide structures using body-of-revolution finite difference time domain method," *Microwave and Optical Technology Letters*, vol. 49, no. 9, pp. 467 – 469, Sept. 2007.

[3] A. Rolland, "*Conception d'antennes métallo-diélectriques par optimisation globale basée sur le couplage entre la méthode FDTD et les algorithmes génétiques*," These de Doctorat, Universite de Rennes 1, Jan. 2009.

[4] Yee, K. S., "Numerical solution of initial boundary value problems involving Maxwell's equations in isotropic media," *IEEE Trans. Antennas and Propagation*, vol. 14, 1966, pp. 302-307.

[5] M. Celuch and W. K. Gwarek, "Industrial design of axis-symmetrical devices using a customized solver from RF to optical frequency bands," *IEEE Microwave Mag.*, vol. 9, no. 6, pp. 150 – 159, Dec. 2008.

[6] A. Taflove and S. C. Hagness, *Computational Electrodynamics: the Finite-Difference Time-Domain Method*, 2nd ed., Artech House, Inc., 2000.

[7] S. H. Dahlan, A. Rolland, R. Sauleau, "Application of the dual-grid scheme in BoR FDTD for the simulation of dual reflector antennas", *European Conf. on Antennas and Propagation, EuCAP 2011*, pp. 1345-1348, Rome, Italy, 11-15 Apr. 2011.

[8] S. H. Dahlan, A. Rolland, R. Sauleau, "Schémas d'analyse rapide de problèmes axisymétriques par la méthode FDTD à symétrie de révolution (BoR-FDTD)", *Dix-septièmes Journées Nationales Micro-ondes*, Brest, 4 pages, 18-20 May 2011.

[9] S. A. Muhammad, A. Rolland, S. H. Dahlan, R. Sauleau and H. Legay, "Comparison between Scrimp horns and stacked Fabry-Perot cavity antennas with small apertures," *European Conf. on Antennas and Propagation, EuCAP 2012*, (Submitted).

[10] Romain Pascaud, "Nouveaux schémas rapides pour la méthode des Différences Finies dans le Domaine Temporel (FDTD). Application à la simulation d'antennes environnées," Thèse de Doctorat, Institut National des Sciences Appliquées de Rennes, Dec. 2007.

Chapter 2

The Finite Difference Time Domain Method – General Overview

2.1 Method principle

Time-varying electric and magnetic fields bond together into inseparable quantities by means of electromagnetics theory. Not until before the middle of the 19th century, both electric and magnetic fields were recognized to be independent to each other. The later extensive study of electricity and magnetism leads to the relation of the motion of both physical quantities, explained particularly through the Ampere's and Faraday's law. These discoveries together with others were unified by James Clerk Maxwell in 1873 through his famous publication, *Treatise on Electricity and Magnetism*, in which he elegantly constructed four mathematical equations, now well known as the Maxwell's Equations. They were explained in set of four vector differential equations with four vector quantities:

$$\vec{\nabla} \times \vec{H} = \varepsilon \frac{\partial \vec{E}}{\partial t} + \vec{J} \tag{2.1}$$

$$\vec{\nabla} \times \vec{E} = -\mu \frac{\partial \vec{H}}{\partial t} \tag{2.2}$$

$$\vec{\nabla} \cdot \vec{B} = 0 \tag{2.3}$$

$$\vec{\nabla} . \vec{D} = \rho \tag{2.4}$$

where

H - magnetic field intensity (A/m),

E - electric field intensity (V/m),

J - electric current density (A/m^2),

B - magnetic flux density (Wb/m^2),

D - electric flux density (C/m^2),

ρ - electric charge density (C/m^3),

ε - permittivity (F/m),

μ - permeability (H/m).

Electric and magnetic fields are considered as separated and static by Gauss law (2.3) - (2.4) while the time-varying properties of the fields are described by Ampere's (2.1) and Faraday's law (2.2). The time-dependent equations were set into a finite difference scheme [1]. Through the scheme, the field components are arranged in a special cubic arrangement called the Yee cell (Figure 2.1) (introduced by Kane Yee in 1966) [2]. Such arrangement allows for the solution of the Maxwell's curl equations in the following discretized form, with second-order accuracy and considering the fields are in free space:

$$E_x^{n+1}(i,j,k) = E_x^n(i,j,k) + \left(H_z^{n+\frac{1}{2}}\left(i,j+\frac{1}{2},k\right) - H_z^{n+\frac{1}{2}}\left(i,j-\frac{1}{2},k\right)\right)\frac{\Delta t}{\varepsilon_0 \Delta y} + \left(H_y^{n+\frac{1}{2}}\left(i,j,k-\frac{1}{2}\right) - H_y^{n+\frac{1}{2}}\left(i,j,k+\frac{1}{2}\right)\right)\frac{\Delta t}{\varepsilon_0 \Delta z} \tag{2.5}$$

$$E_y^{n+1}(i,j,k) = E_y^n(i,j,k) + \left(H_x^{n+\frac{1}{2}}\left(i,j,k+\frac{1}{2}\right) - H_x^{n+\frac{1}{2}}\left(i,j,k-\frac{1}{2}\right)\right)\frac{\Delta t}{\varepsilon_0 \Delta z} + \left(H_z^{n+\frac{1}{2}}\left(i-\frac{1}{2},j,k\right) - H_z^{n+\frac{1}{2}}\left(i+\frac{1}{2},j,k\right)\right)\frac{\Delta t}{\varepsilon_0 \Delta x} \tag{2.6}$$

$$E_z^{n+1}(i,j,k) = E_z^n(i,j,k) + \left(H_y^{n+\frac{1}{2}}\left(i+\frac{1}{2},j,k\right) - H_y^{n+\frac{1}{2}}\left(i-\frac{1}{2},j,k\right)\right)\frac{\Delta t}{\varepsilon_0 \Delta x} + \left(H_x^{n+\frac{1}{2}}\left(i,j-\frac{1}{2},k\right) - H_x^{n+\frac{1}{2}}\left(i,j+\frac{1}{2},k\right)\right)\frac{\Delta t}{\varepsilon_0 \Delta y} \tag{2.7}$$

$$H_x^{n+\frac{1}{2}}(i,j,k) = H_x^{n-\frac{1}{2}}(i,j,k) + \left(E_y^n\left(i,j,k+\frac{1}{2}\right) - E_y^n\left(i,j,k-\frac{1}{2}\right)\right)\frac{\Delta t}{\mu_0 \Delta z} + \left(E_z^n\left(i,j-\frac{1}{2},k\right) - E_z^n\left(i,j+\frac{1}{2},k\right)\right)\frac{\Delta t}{\mu_0 \Delta y} \tag{2.8}$$

$$H_y^{n+\frac{1}{2}}(i,j,k) = H_y^{n-\frac{1}{2}}(i,j,k) + \left(E_z^n\left(i+\frac{1}{2},j,k\right) - E_z^n\left(i-\frac{1}{2},j,k\right)\right)\frac{\Delta t}{\mu_0 \Delta x} + \left(E_x^n\left(i,j,k-\frac{1}{2}\right) - E_x^n\left(i,j,k+\frac{1}{2}\right)\right)\frac{\Delta t}{\mu_0 \Delta z} \tag{2.9}$$

$$H_z^{n+\frac{1}{2}}(i,j,k) = H_z^{n-\frac{1}{2}}(i,j,k) + \left(E_x^n\left(i,j+\frac{1}{2},k\right) - E_x^n\left(i,j-\frac{1}{2},k\right)\right)\frac{\Delta t}{\mu_0 \Delta y} + \left(E_y^n\left(i-\frac{1}{2},j,k\right) - E_y^n\left(i+\frac{1}{2},j,k\right)\right)\frac{\Delta t}{\mu_0 \Delta x} \tag{2.10}$$

where

Δt	-	time step,
n	-	time step index,
$\Delta x, \Delta y, \Delta z$	-	cell dimensions,
(i,j,k)	-	cell indices.

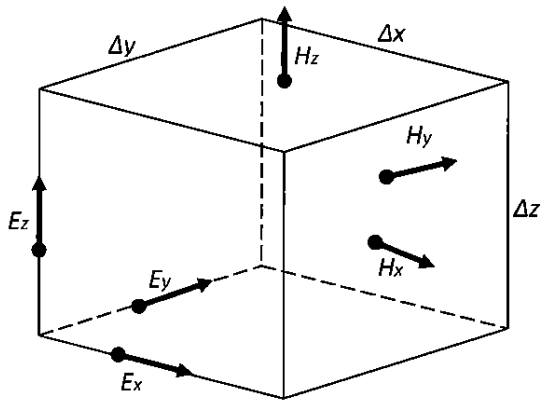

Figure 2.1 - Yee cell concept in FDTD.

Equation (2.5) – (2.10) form the basis for the finite-difference time-domain (FDTD) computational scheme. The magnetic and electric field components are computed in consecutive time instants, every half of a time step Δt, forming a leapfrog time-stepping algorithm. Stability of the FDTD method is relevant to the spatial grid size and the time-step relation. The so called Courant stability criterion must be satisfied to keep the stability of the algorithm:

$$p \geq \sqrt{3} \tag{2.11}$$

where

$$p = \frac{1}{c\Delta t}\sqrt{\frac{3}{\Delta x^{-2} + \Delta y^{-2} + \Delta z^{-2}}} \tag{2.12}$$

is a stability coefficient.

To maintain algorithm stability, the applied time step has to be small enough for the specified spatial grid. Otherwise, the physical velocity of the considered EM wave being faster than the numerical speed of the FDTD algorithm resulting a shift of the numerically propagating amplitude at the wave front.

Another inherent property of the FDTD method related to the spatial discretization is the numerical dispersion, which could limit the algorithm accuracy. It explains why the

physical velocity of a wave differs from the velocity of a numerically propagated wave and this discrepancy is frequency and direction-dependent. This inaccuracy is due to the numerical dispersion which is inversely proportional to the square of the spatial grid. In practice, one should set at least 10 FDTD cells per wavelength to keep the numerical dispersion below about 1.5% [3]. In most cases, it is often required to set the cell at even greater than 20 cells per wavelength for better accuracy.

In terms of computational capabilities, the FDTD method requires $X*N^3$ floating point operations, where X stands for the number of cells along one side of the considered computational space. Generally each cell comprises of 6 field components, the total number of variable to be stored in the memory is approximately $6*N^3$. For an example, assuming that each component requires 4 bytes, a computational space comprising 100x100x100 FDTD cells requires at least 24MB of operating memory. Additional refinement of the FDTD spatial grid by 2 requires $2^3=8$ times more operating memory. This as well increases the computation time by $2^4=16$ times. Thus through the manipulation of the FDTD cell size, it could leads to saving lots of computational resources. This indicates that the trade-off between simulation time and accuracy plays an important role in electromagnetic modeling when using the FDTD method.

The basic FDTD algorithm alone is limited to the calculation of the propagating electromagnetic wave. This however can be enhanced by adding some numerical tools that can extends its capability and scopes which is especially important to the application of antenna and other similar electromagnetic problems. Some of the additional tools and features are:

1. The absorbing boundary condition (ABC)

   The ABC allows for modeling a radiation problem of an FDTD model out to a free-space. There are two types of commonly used technique for the purpose; the perfectly matched layer (PML) [4] and the Mur approach [5]. The PML introduces additional unphysical quantities and comprises only a few FDTD layers, shrinking the overall calculation size. It is not so much angle-dependent and can be placed close to radiating sources without the risk of instability. The Mur ABC on the other hand could produce instability when dealing with propagation of an electromagnetic wave at grazing angles especially in resonant structures. This

effect however could be reduced by implementation of some extension technique called the Mur superabsorbation [6] which is much less sensitive to variation of an incident angle. The major property of the Mur ABC is that it can accurately matched incoming wave at a particular direction, by changing the effective permittivity of the Mur absorption. This property will deteriorates to some extent for incoming wave at angles different compared to the matched one.

2. The total field-scattered field (TF-SF) decomposition

   This technique is very useful in antenna and radar analysis. The FDTD problem space is divided into two separate regions by virtual TF-SF boundaries which then known as the total field (TF) region and the scattered field (SF) region [3]. An incident plane wave is excited inside the total field region. It can be a direct or an oblique plane wave depending on the problem analysis. Whenever there is no scatterer or obstacle in the TF region, the applied incident plane wave will not radiate outside the TF region into the SF region. On the other hand, with the present of obstacle inside the TF region, only the scattered part of the electromagnetic wave will be radiated outside the region into the SF region.

3. Near-field to far-field transformation (NTFF)

   An important technique for calculating the far field characteristics of a radiating source based on the near field information without having to extend the radiation space to the far field region. The near-to-far field transformation is performed around a surrounding transformation surface enclosing the radiating source in the near field region. It is a post-processing technique that calculates the contributions of the radiated fields over time for gaining the far field information either in time or frequency domain. It is widely applied in antenna design [7].

4. Media

   Media such as lossless/lossy, linear/nonlinear, isotropic/nonisotropic and dispersive/nondispersive can be treated using the FDTD method. Nonlinear media can be treated naturally in FDTD since it is a time-domain approach. For dispersive media, special model such as the Debye, Drude and Lorentz models [3] are commonly applied to represent the characteristic. A single FDTD run could provide results for the whole spectrum range.

5. Mode excitation

   For cylindrical or rectangular waveguide applications, special mode of excitation usually applied, and it is possible to introduce a surface that excites a particular distribution of magnetic and electric tangential field components in FDTD. It can also be applied to waveguide with arbitrary shapes with inhomogeneous filling.

2.2 Some advantages and disadvantages

Briefly, some of major advantages of FDTD can be mentioned:

1. Wideband analysis

   FDTD is a time-domain based algorithm which offers a wideband analysis with only one simulation run. Even though this require an additional post processing but it can be done while performing the iterative run (on the fly) [3] with very low computation effort.

2. Intuitive algorithm

   Propagation of wave can be monitored in time domain enables ones to have good understanding of the considered problem behavior while performing a study. It offers a fast and accurate feedback for better decision making and give early information for possible potential problems of a design.

3. Unconditional stability

   The FDTD algorithm is unconditionally stable provided that the Courant stability criterion is satisfied.

However, like other numerical modeling method, the FDTD method has some limitations. Some of them are briefly mentioned here:

1. Physical geometry approximation

   When dealing with complex geometry some features in the design sometimes requires very fine geometrical details and cannot be neglected. The FDTD cell size needed for handling this geometry features are unavoidably very small. This increase the computation time substantially. However, there are methods that

could handle this efficiently in FDTD such as by applying the multi-resolution approach. In this thesis a new multi-resolution approach based on the dual grid method is introduced in the subsequent chapter for handling such issue in the bodies of revolutions FDTD (BoR-FDTD) environment. The explanation about BoR-FDTD is detailed in the next chapter.

2. Long computation of high-Q structures

   Performing simulation for a high-Q structure using the time domain approach might require very long computation time. This is due to the slow field dissipations. The problem can be more challenging when involving finer resolution in time and space. This issue however is not only restricted to FDTD alone but other analysis methods are also face similar problem.

2.3 Conclusion

In summary, a brief discussion of the general FDTD method has been presented. Some of its major properties as well as its inherent limitations have been pointed out. Next chapter will present the bodies of revolution (BoR) FDTD, a FDTD approach based on cylindrical coordinate system to handle axis-symmetrical electromagnetic problems. The BoR-FDTD is the main method used throughout this work.

References

[1] Taflove. A., and M. E. Brodwin, "Numerical solution of steady-state electromagnetic scattering problems using the time-dependent Maxwell's equations," *IEEE Trans. Microwave Theory and Techniques*, vol. 23, 1975, pp. 623-630.

[2] Yee, K. S., "Numerical solution of initial boundary value problems involving Maxwell's equations in isotropic media," *IEEE Trans. Antennas and Propagation*, vol. 14, 1966, pp. 302-307.

[3] A. Taflove, "Computational Electrodynamics: The Finite-Difference Time-Domain Method", Artech House, 1995.

[4] J. P. Berenger, "A perfectly matched layer for the absorption of electromagnetic waves," *J. Comput. Phys.*, vol. 114, no. 2, pp. 185-200, Oct. 1994.

[5] G. Mur, "Absorbing boundary conditions for the finite-difference approximation of the time-domain electromagnetic-field equations," *IEEE Trans. Electromagnetic Compatibility*, vol. EMC-23, no. 4, pp. 377-382, Nov. 1981.

[6] K. K. Mei., J. Fana, "Superabsorption – A method to improve absorbing boundary conditions," *IEEE Trans. Antennas & Propagat.*, vol. AP-40, pp. 1001-1010, Sept. 1992.

[7] C. A. Balanis, *Antenna Theory Analysis and design*, 2nd ed., John Wiley & Sons, Inc., 1997.

Chapter 3

Bodies of Revolution Finite Difference Time Domain (BoR-FDTD) Simulator

3.1 Introduction

Bodies of revolution (BoR) or rotationally symmetric structures are commonly encountered in many electromagnetic problems such as on the axis-symmetrical reflectors [1], lens antennas [2][3] and conical horns [4][5]. This chapter presents the BoR FDTD algorithm for modeling such structures. Naturally, the cylindrical coordinates system is used to describe them most efficiently. Furthermore the azimuthal dependence of the fields can be expressed analytically by using the Fourier series. Thus the space discretization in this direction is unnecessary. Therefore the 3-dimensional (3D) Yee cell in cylindrical coordinates (ρ,φ,z) can be projected into the 2-dimensional (2D) cell in the (ρ,z) plane, allowing reduction of computer resources usage as well as saving in computation time [6].

The first part of the chapter will concentrate on the presentation of the 2D BoR-FDTD algorithm for computations of space in cylindrical coordinate system, including the derivations of the governing equations and the discretization of the update equations. Then the approach to handle singularities for field components along the symmetrical axis will be discussed together with the stability criteria. Method for additional tools that important for antenna studies such as the truncation of space for the absorbing boundary conditions using the unified perfectly matched layer (U-PML), system excitations and the near to far field transformation method are discussed in the second part. Finally, the algorithm and the additional tools have been put together for the development of a BoR-FDTD simulator [5]. The work flow of the simulator is presented, showing the steps taken for performing electromagnetic simulation work.

3.2 Specification and presentation of BoR-FDTD method

3.2.1 The governing equations

The BoR structures are symmetric about the axis and this leads to the natural use of the cylindrical coordinates (ρ,φ,z) as illustrated in Figure 3.1.

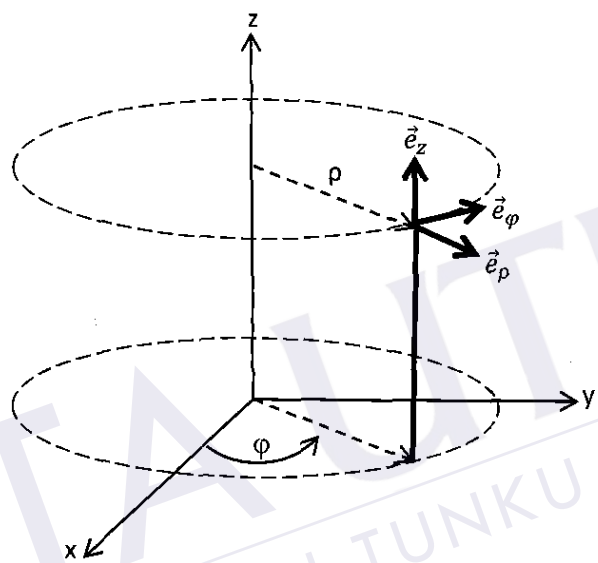

Figure 3.1 - Cylindrical coordinate system.

To derive the governing equations for the BoR-FDTD we should go back to the Maxwell curl equations given in (2.1) to (2.2) from the previous chapter. In cylindrical coordinates system, the Maxwell equations can be rewritten as:

$$\frac{1}{\rho}\begin{bmatrix} 0 & -\rho\partial_z & \partial_\varphi \\ \rho\partial_z & 0 & -\rho\partial_\rho \\ -\partial_\varphi & \partial_\rho\rho & 0 \end{bmatrix}\begin{bmatrix} E_\rho \\ E_\varphi \\ E_z \end{bmatrix} = -\mu_0\begin{bmatrix} \mu_\rho & 0 & 0 \\ 0 & \mu_\varphi & 0 \\ 0 & 0 & \mu_z \end{bmatrix}\cdot\begin{bmatrix} \frac{\partial H_\rho}{\partial t} \\ \frac{\partial H_\varphi}{\partial t} \\ \frac{\partial H_z}{\partial t} \end{bmatrix} \tag{3.1}$$

$$\frac{1}{\rho}\begin{bmatrix} 0 & -\rho\partial_z & \partial_\varphi \\ \rho\partial_z & 0 & -\rho\partial_\rho \\ -\partial_\varphi & \partial_\rho\rho & 0 \end{bmatrix}\begin{bmatrix} H_\rho \\ H_\varphi \\ H_z \end{bmatrix} = \varepsilon_0\begin{bmatrix} \varepsilon_\rho & 0 & 0 \\ 0 & \epsilon_\varphi & 0 \\ 0 & 0 & \varepsilon_z \end{bmatrix}\begin{bmatrix} \frac{\partial E_\rho}{\partial t} \\ \frac{\partial E_\varphi}{\partial t} \\ \frac{\partial E_z}{\partial t} \end{bmatrix} + \begin{bmatrix} \sigma_\rho^e & 0 & 0 \\ 0 & \sigma_\varphi^e & 0 \\ 0 & 0 & \sigma_z^e \end{bmatrix}\begin{bmatrix} E_\rho \\ E_\varphi \\ E_z \end{bmatrix} \tag{3.2}$$

where

$\mu = \begin{bmatrix} \mu_\rho & 0 & 0 \\ 0 & \mu_\varphi & 0 \\ 0 & 0 & \mu_z \end{bmatrix}$ denotes the relative permeability tensor,

$\varepsilon = \begin{bmatrix} \varepsilon_\rho & 0 & 0 \\ 0 & \varepsilon_\varphi & 0 \\ 0 & 0 & \varepsilon_z \end{bmatrix}$ represents the relative permittivity tensor,

$\sigma = \begin{bmatrix} \sigma_\rho^e & 0 & 0 \\ 0 & \sigma_\varphi^e & 0 \\ 0 & 0 & \sigma_z^e \end{bmatrix}$ is the electric conductivity of the medium tensor,

ε_0 and μ_0 are the free-space permittivity and permeability respectively.

Expanding equations (3.1) and (3.2) in linear form, we obtain:

$$\frac{\partial E_\varphi}{\partial_z} - \frac{1}{\rho}\frac{\partial E_z}{\partial_\varphi} = \mu_0\mu_\rho\frac{\partial H_\rho}{\partial t} \tag{3.3}$$

$$-\frac{\partial E_\rho}{\partial_z} + \frac{\partial E_z}{\partial_\rho} = \mu_0\mu_\varphi\frac{\partial H_\varphi}{\partial t} \tag{3.4}$$

$$\frac{1}{\rho}\frac{\partial E_\rho}{\partial\varphi} - \frac{1}{\rho}\frac{\partial(\rho E_\varphi)}{\partial\rho} = \mu_0\mu_z\frac{\partial H_z}{\partial t} \tag{3.5}$$

$$-\frac{\partial H_\varphi}{\partial z} + \frac{1}{\rho}\frac{\partial H_z}{\partial\varphi} = \varepsilon_0\varepsilon_\rho\frac{\partial E_\rho}{\partial t} + \sigma_\rho^e E_\rho \tag{3.6}$$

$$\frac{\partial H_\rho}{\partial z} - \frac{\partial H_z}{\partial \rho} = \varepsilon_0 \varepsilon_\varphi \frac{\partial E_\varphi}{\partial t} + \sigma_\varphi^e E_\varphi \tag{3.7}$$

$$-\frac{1}{\rho}\frac{\partial H_\rho}{\partial \varphi} + \frac{1}{\rho}\frac{\partial (\rho H_\varphi)}{\partial \rho} = \varepsilon_0 \varepsilon_z \frac{\partial E_z}{\partial t} + \sigma_z^e E_z \tag{3.8}$$

From equation (3.3) to (3.8) it can be noted that the cylindrical space is discretized in three dimensional manners along the ρ, φ, and z directions. However, thanks to the rotationally symmetric structures where fields variations in the azimuthal (φ) directions can be solved analytically. In order to do that, we first expand the electric and magnetic fields in the rotationally symmetric geometries using the infinite Fourier series expansion [6], [8]. It is written as:

$$\vec{E}(\rho, \varphi, z; t) = \sum_{m=0}^{\infty} \left[\vec{E}(\rho, z; t)_{even} cos(m\varphi) + \vec{E}(\rho, z; t)_{odd} sin(m\varphi)\right] \tag{3.9}$$

$$\vec{H}(\rho, \varphi, z; t) = \sum_{m=0}^{\infty} \left[\vec{H}(\rho, z; t)_{even} cos(m\varphi) + \vec{H}(\rho, z; t)_{odd} sin(m\varphi)\right] \tag{3.10}$$

where m is the azimuthal mode number. The subscript *even* and *odd* denotes the Fourier coefficients for the cosinusoidal or sinusoidal dependence respectively. Originally the electric and magnetic fields are a function of ρ, φ and z at all time. However, once expanded in Fourier series, the fields are now dependent only on ρ and z components but varied with *cos(mφ)* and *sin(mφ)*.

Without losing generality, we can now assume that the angular variation of the electromagnetic fields has either a *cos(mφ)* or *sin(mφ)* variation. In our case we choose the field variations as:

$$E_\rho, E_z, H_\varphi \sim \sin(m\varphi) \tag{3.11}$$

$$H_\rho, H_z, E_\varphi \sim \cos(m\varphi) \tag{3.12}$$

By applying the Fourier expansion series of (3.9) and (3.10) into the time domain equation (3.3) to (3.8) together with definition used in (3.11) and (3.12), the three-dimensional problem of the fields in cylindrical coordinate can now be simplified into a two dimensional one. Thus, the time domain equation (3.3) to (3.8) can be reduced as set of six equations:

$$\frac{\partial E_\varphi(\rho,z;t)}{\partial z}-\frac{m}{\rho}E_z(\rho,z;t)=\mu_0\mu_\rho\frac{\partial H_\rho(p,z;t)}{\partial t} \tag{3.13}$$

$$-\frac{\partial E_\rho(\rho,z;t)}{\partial z}+\frac{\partial E_z(\rho,z;t)}{\partial \rho}=\mu_0\mu_\varphi\frac{\partial H_\varphi(\rho,z;t)}{\partial t} \tag{3.14}$$

$$\frac{m}{\rho}E_\rho(\rho,z;t)-\frac{1}{\rho}\frac{\partial\left(\rho E_\varphi(\rho,z;t)\right)}{\partial \rho}=\mu_0\mu_z\frac{\partial H_z(\rho,z;t)}{\partial t} \tag{3.15}$$

$$-\frac{\partial H_\varphi(\rho,z;t)}{\partial z}-\frac{m}{\rho}H_z(\rho,z;t)=\varepsilon_0\varepsilon_\rho\frac{\partial E_\rho(\rho,z;t)}{\partial t}+\sigma_\rho^e E_\rho(\rho,z;t) \tag{3.16}$$

$$\frac{\partial H_\rho(\rho,z;t)}{\partial z}-\frac{\partial H_z(\rho,z;t)}{\partial \rho}=\varepsilon_0\varepsilon_\varphi\frac{\partial E_\varphi(\rho,z;t)}{\partial t}+\sigma_\varphi^e E_\varphi(\rho,z;t) \tag{3.17}$$

$$\frac{m}{\rho}H_\rho(\rho,z;t)+\frac{1}{\rho}\frac{\partial\left(\rho H_\varphi(\rho,z;t)\right)}{\partial \rho}=\varepsilon_0\varepsilon_z\frac{\partial E_z(\rho,z;t)}{\partial t}+\sigma_z^e E_z(\rho,z;t) \tag{3.18}$$

In these equations, for any given mode number m, the azimuthal variation are now analytically accounted for and hence discretization in φ direction is no longer necessary. Equations (3.13) to (3.18) are only dependent on space discretization in ρ and z direction together with the time dimensions. Reduction from three dimensional to two dimensional problems can significantly reduce computer resources as well as the required computational time. This forms the major advantage of the algorithm as whole. These are the equations that

govern the electromagnetic fields in bodies of revolution (BoR) structure in its normal FDTD computational space.

3.2.2 Discretization of the governing equations

3.2.2.1 Gridding scheme in three dimensional cylindrical coordinate

The governing equations need to be discretized for used in the FDTD scheme and the update equations must be derived based on the grid definition. In the FDTD method the electric field and the magnetic fields are located at offset position from one another in the designated space. For reference, the general three dimensional FDTD cell in cylindrical coordinate system is as illustrated in Figure 3.2. The positions of all electric field components are at the cell borders tangential to each other and effectively located half cells apart from the reference point (i,j,k). The magnetic fields components on the other hand are defined normally to the surface of the cylindrical cell and are half cells apart from the electric fields in the cell.

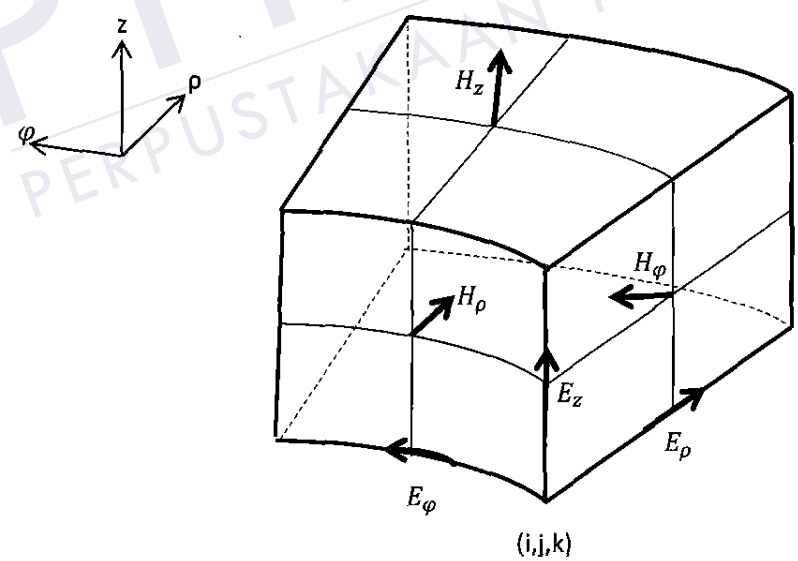

Figure 3.2 - The three dimensional FDTD cell in cylindrical coordinates.

3.2.2.2 Gridding scheme for the BoR-FDTD

As the fields are now in two dimensional space, they form a unique arrangement on the ρ-z plane. By looking at the fields from a cut plane, all six field components can be viewed in their unique position. That is because even though the computation space is in two dimensional, the physical electromagnetic fields are still in three dimensional in nature. For better understanding, Figure 3.3 illustrates the off-axis field position and the arrangement on the plane.

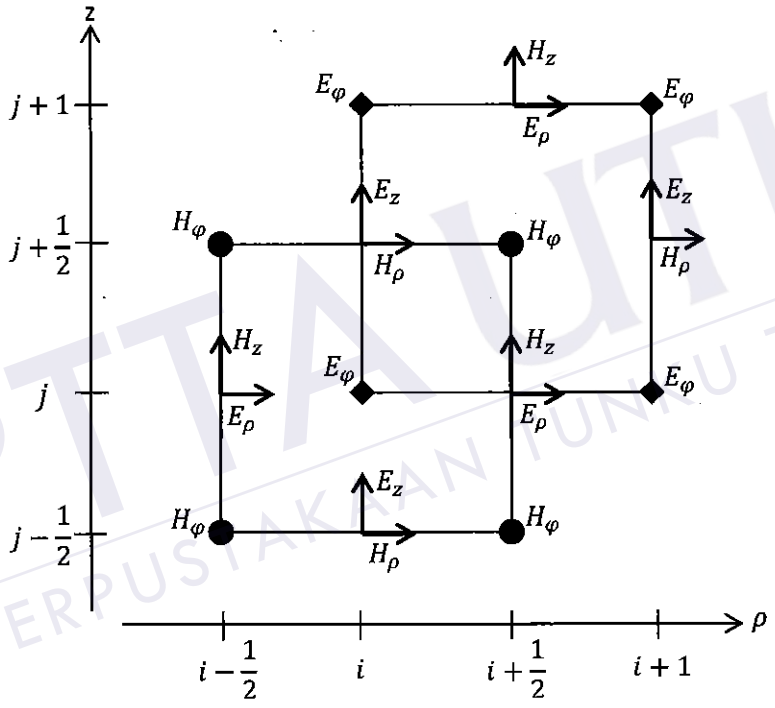

Figure 3.3 – Arrangement of field components in 2D plane in cylindrical coordinates.

It can be noted for field components $\{H_z, E_\rho\}$ and $\{E_z, H_\rho\}$, they seem to be located at the same exact position. However they are actually half cells apart from each other and this can be seen more clearly from the three dimensional illustration as in Figure 3.2.

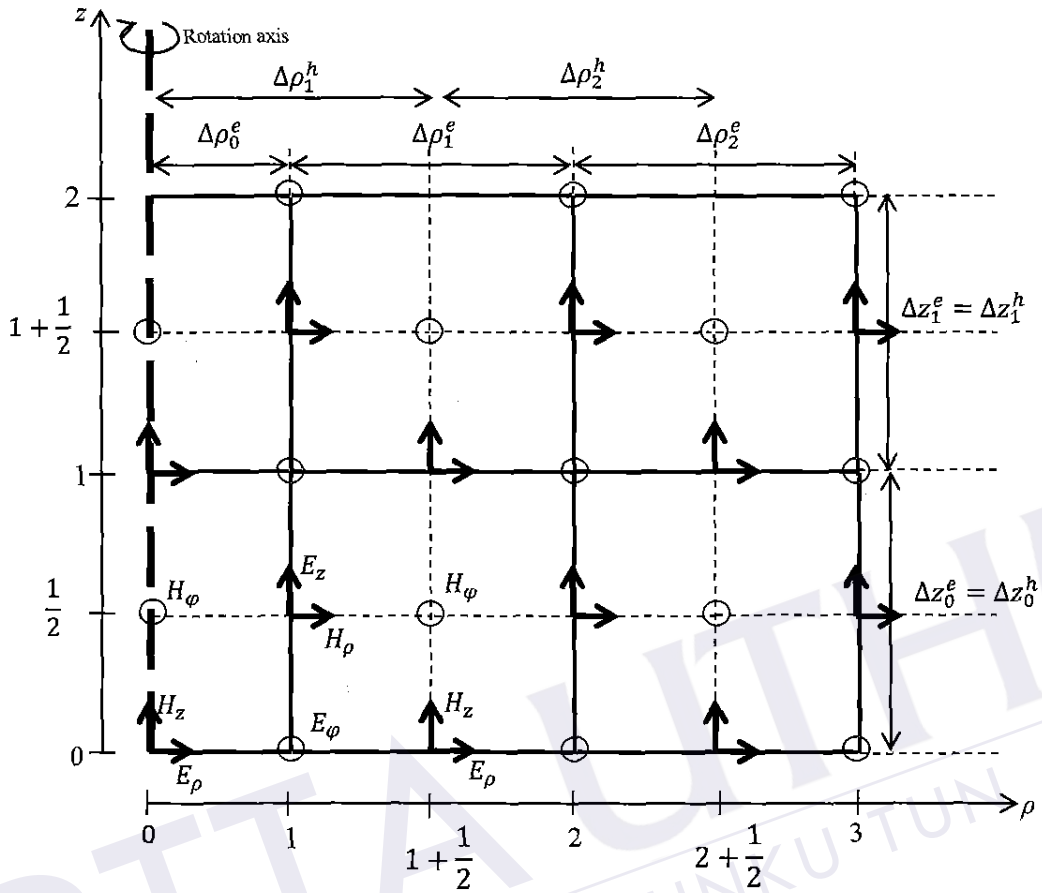

Figure 3.4 – Cell definitions on the BoR-FDTD grid system

From Figure 3.4, we show some cells and field components on the BoR-FDTD grid system. The definitions of the cell sizes and the half cells are given. Note that BoR-FDTD lattice has uniform size in z direction but distributed non-uniformly in ρ direction. The following defines the cell sizes and half cells coordinate for both directions:

$$\rho_0 = 0\ ,\ \rho_{\frac{1}{2}} = 0 \tag{3.19}$$

$$\Delta\rho_i^e = \rho_{i+1} - \rho_i \text{ for } \quad i = 0 \sim N_\rho - 1 \tag{3.20}$$

$$\rho_{i+1/2} = \rho_i + \Delta\rho_i^e/2 \quad \text{for} \quad i = 1 \sim N_\rho - 1 \tag{3.21}$$

$$\Delta z_j^e = z_{j+1} - z_j \quad \text{for} \quad j = 0 \sim N_z - 1 \tag{3.22}$$

$$z_{j+1/2} = z_j + \Delta z_j^e/2 \quad \text{for} \quad j = 0 \sim N_z - 1 \tag{3.23}$$

$$\Delta\rho_1^h = \Delta\rho_0^e + \frac{\Delta\rho_1^e}{2} \tag{3.24}$$

$$\Delta\rho_i^h = (\Delta\rho_i^e + \Delta\rho_{i-1}^e)/2 \quad \text{for} \quad i = 2 \sim N_\rho - 1 \tag{3.25}$$

$$\Delta\rho_1^h = 2 \times \Delta\rho_0^e \tag{3.26}$$

$$\Delta z_j^h = \left(\Delta z_j^e + \Delta z_{j-1}^e\right)/2 \quad \text{for} \quad j = 1 \sim N_z - 1 \tag{3.27}$$

where N_ρ and N_z are the total number of cells along ρ axis and z axis respectively. These definitions will be used in the update equations where superscript e and h in the equations will refer to electric and magnetic field respectively.

3.2.2.3 Update equations of the BoR-FDTD method

The update equations for the BoR-FDTD are derived by discretizing the governing equations (3.13) to (3.18) through approximations of spatial and time derivatives with the central finite difference. As similar to conventional FDTD scheme, the approximation is second-order accurate in both time and space [8]. The updating process in time requires that the electric and magnetic field to be updated at staggered half time-steps, one after another in leap-frogging manner. Meaning that at a time step, the value of the electric and magnetic fields will dependent on those values at previous time-step and half-time step. For the fields arrangement in space, it requires that both electric and magnetic fields to be off-set from one another. Through this technique a full-wave simulation can be achieved in just one computational run.